

The Journal of Undergraduate Research

Volume 6 *Journal of Undergraduate Research*, Volume
6: 2008

Article 6

2008

Erosion Function Apparatus

Ryan Larsen
South Dakota State University

Follow this and additional works at: <http://openprairie.sdstate.edu/jur>

 Part of the [Environmental Engineering Commons](#)

Recommended Citation

Larsen, Ryan (2008) "Erosion Function Apparatus," *The Journal of Undergraduate Research*: Vol. 6, Article 6.
Available at: <http://openprairie.sdstate.edu/jur/vol6/iss1/6>

This Article is brought to you for free and open access by Open PRAIRIE: Open Public Research Access Institutional Repository and Information Exchange. It has been accepted for inclusion in The Journal of Undergraduate Research by an authorized administrator of Open PRAIRIE: Open Public Research Access Institutional Repository and Information Exchange. For more information, please contact michael.biondo@sdstate.edu.

EROSION FUNCTION APPARATUS

Author: Ryan Larsen
Faculty Sponsor: Dr. Allen Jones, Dr. Francis Ting
Department: Civil and Environmental Engineering

ABSTRACT

The Erosion Function Apparatus (EFA) test uses site-specific soil samples acquired via thin-walled tubes to generate the erosion rate and shear stress which is plotted to create an erosion plot. The information produced by the test can help an engineer accurately determine the depth of scour as a function of time for bridge design, and thereby determine the depth a foundation system should be constructed.

During EFA testing, a data acquisition system records the velocity and amount of soil eroded. This data is used to calculate the Reynolds Number, friction factor, erosion rate, and shear stress. Once the data has been reduced to erosion rate and shear stress, it is plotted to form an EFA plot.

The EFA test contains significant uncertainties in selecting the roughness values and timing of the test. Selecting incorrect roughness values can produce a misleading EFA plot by incorrectly calculating the shear stresses, which will not be representative of the erodibility of the soil. Incorrectly timing the test will also lead to an inaccurate representation of the erodibility of the soil by improperly calculating the erosion rate.

INTRODUCTION

Soil scour around a bridge pier is a major design consideration for bridge design. A major cost of constructing a bridge results from the depth of the foundations needed to resist soil scour resulting from water turbulence as water flows around a pier. The deeper the foundation, the more expensive the bridge; therefore, if scour depth is determined by conservative methods and is used as the design depth for the foundation, the bridge may be over-designed. The maximum scour depth may never develop during the lifetime of a bridge if the in-situ soil is clay or silt (Ting et. al. 2001); therefore, it is appropriate to accurately predict the scour rate for the foundation's depth.

Scour rate in coarse-grained soils is well understood and easy to calculate since one major flood event can cause the maximum scour depth. A coarse-grained soil will erode very evenly and quickly because the only force that resists erosion is the friction between the grains. Since the soil will erode quickly and the maximum scour depth will likely be reached during the lifetime of the bridge, an engineer can use the maximum scour depth as the design depth.

Fine-grained soils present a much more difficult analysis due to the forces that develop between the individual particles (Briaud et. al. 2001). Isomorphous substitution and defects in the particle crystals cause clays to have a negative surface charge. The

negative charge attracts water molecules to the surface of the particle until it has a thin layer of water surrounding it. Each fine-grained particle has this same attraction to water molecules, and the water molecules in turn are attracted to each other forming a weak hydrogen bond. Due to the hydrogen bonding, the engineering behavior is much different for fine-grained soils. They erode very irregularly and slower than coarse-grained soils; therefore, a bridge may never experience the maximum scour depth within its design life. Because of this slower erosion rate, it is essential to understand and predict the scour rate for fine-grained soils in order to determine an appropriate design depth for foundations. The EFA was created as a means to determine the erosion rate in fine-grained soils.

Each soil will have a unique initial stress where the soil begins to erode, termed the critical shear stress and erosion rate, which are essential to predicting the scour depth. Shear stress is directly proportional to the fluid velocity at the soil/water interface. The EFA allows for the determination of the critical shear stress and the erosion rates at several other shear stresses by increasing the flow velocity and timing how quickly the soil erodes.

The result from the EFA test is used as input into a newly developed method of determining the scour depth around a pier over time. This new method and the developmental process is discussed in detail in engineering journals (Briaud et. al. 1999, 2001 a, b, 2004, and Ting et. al. 2001).

METHOD

The EFA device utilizes site-specific, thin-walled tube samples to acquire an erosion plot. Samples are extracted as close to the foundations as possible. A borehole is drilled to the desired depth, and thin-walled tubes are pushed into the soil. The tube is extracted with the soil sample inside.

The tubes are placed into the device and one millimeter of soil is extruded into a water tunnel. Water enters the tunnel at an initial velocity (generally less than 1.0 m/s), and the operator increases it until soil erosion is observed. A fine-grained soil will generally start to erode at a high velocity (i.e. 3 m/s). It is important to record the critical velocity where the soil begins to erode, since this velocity marks the critical shear stress of the soil.

The velocity is increased incrementally above the critical velocity. At each increment, the sample erodes for a period of time. The amount of erosion and test duration are recorded and are used to calculate the erosion rate.

Between test velocities, the sample is removed from the tunnel, and the soil is trimmed to the top of the tube. As stated before, fine-grained soils (clays and silts) erode very irregularly; the sample must be trimmed in order to accurately determine when 1 mm has eroded for the next desired velocity.

RESULTS

The data from the EFA test is reduced to erosion rate (mm/hr) and shear stress (Pa). The erosion rate is calculated by dividing the amount of soil eroded by the duration of the test. The shear stress is calculated by first calculating the Reynolds Number, $Re = \frac{v \cdot D}{\nu}$ where v =average flow velocity; D =pipe diameter; and ν =kinematic viscosity, and

friction factor, $\frac{1}{\sqrt{f}} = -2.0 \log \left(\frac{\epsilon}{3.7D} + \frac{2.51}{Re\sqrt{f}} \right)$ where f =friction factor and ϵ =mean height of

roughness of pipe. Using Re and f , the shear stress is calculated by $\tau = \frac{1}{8} \cdot \rho \cdot f \cdot v^2$ where τ =shear stress and ρ =density of fluid. The critical shear stress and the other shear stresses are plotted against the erosion rates to create the erosion plot.

Figure 1 represents the erosion plot for a soil sample obtained from a bridge abutment near Big Sioux River, Flandreau, SD. The shear stress was calculated with a constant roughness value of 1 mm. Seven shear stresses above the critical shear stress were calculated from the test velocities.

Figure 2 represents the erosion plot for a soil sample obtained from a bridge abutment near Split-Rock Creek, Brandon, SD. The shear stress was calculated with a constant roughness value of 1 mm. Multiple shear stresses were calculated below the critical shear stress, but only three were calculated above the critical shear stress because of the limited velocity of the apparatus (approximately 6 m/s).

Figure 3 represents the erosion plot for a soil sample obtained from a bridge abutment near White River, Presho, SD. The shear stress was calculated with a constant roughness value of 1 mm. Three shear stresses above the critical shear stress were calculated from the test velocities.

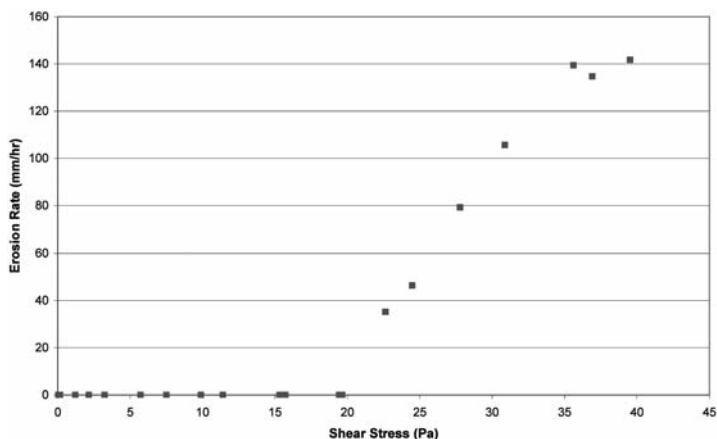


Figure 1. Erosion plot for soil obtained from a bridge abutment near Big Sioux River, Flandreau, SD.

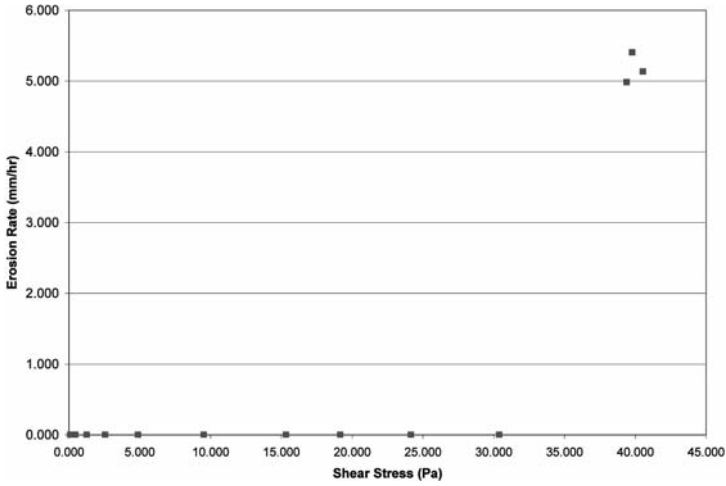


Figure 2. Erosion plot for soil obtained from a bridge abutment near Split-Rock Creek, Brandon, SD.

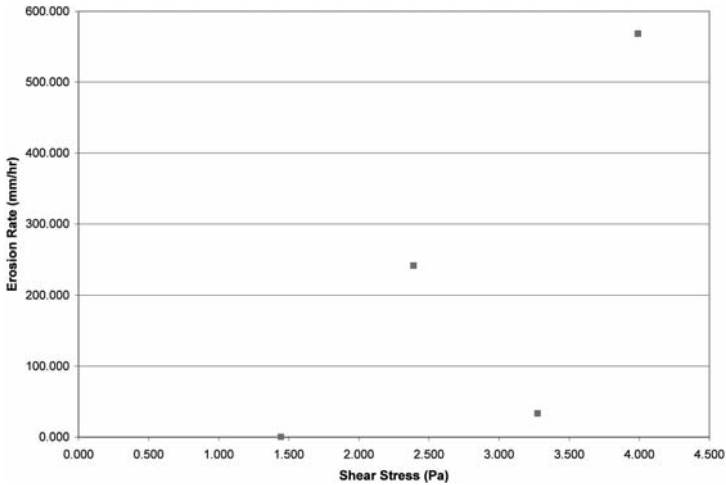


Figure 3. Erosion plot for soil obtained a from bridge abutment near White River, Presho, SD.

DISCUSSION

A site-specific sample is the main advantage of using the EFA method to acquire the erosion plot. Comparing the different erosion plots for the three sites, it is apparent that

the erosion of soils can vary greatly from one location to another. The shear stresses and erosion rates ranged from 40 Pa with a corresponding erosion rate of 5.5 mm/hr to 4.0 Pa with a corresponding erosion rate of 570 mm/hr. Because of this wide variability in soils, a site-specific soil sample is a great asset to acquire an understanding of the erodibility of the site-specific soils.

A large uncertainty is introduced throughout the testing procedure. In order to calculate the shear stresses from the velocity, a friction factor, f , must first be calculated.

The Colebrook formula, $\frac{1}{\sqrt{f}} = -2.0 \log \left(\frac{\epsilon}{3.7D} + \frac{2.51}{\text{Re}\sqrt{f}} \right)$, uses a roughness value, ϵ , to

calculate the friction factor. A constant roughness can be estimated (i.e. 1 mm) or the operator can estimate the roughness of the sample at each test velocity by looking at the soil sample. Because fine-grained soils typically erode very irregularly, a large uncertainty is introduced if the roughness is estimated for each test velocity. A similar uncertainty is introduced if the roughness remains constant for each test, since the chosen roughness may be incorrect for the sample at some test velocities. Estimating a different ϵ value results in a different shear stress, which changes the computed erodibility of the soil at certain shear stresses. Figure 4 shows how the shear stress can change as different roughness values are estimated. With an ϵ value of 0 mm, the critical shear stress is near 7 Pa; however, with an ϵ value of 1 mm, the critical shear stress is near 19 Pa.

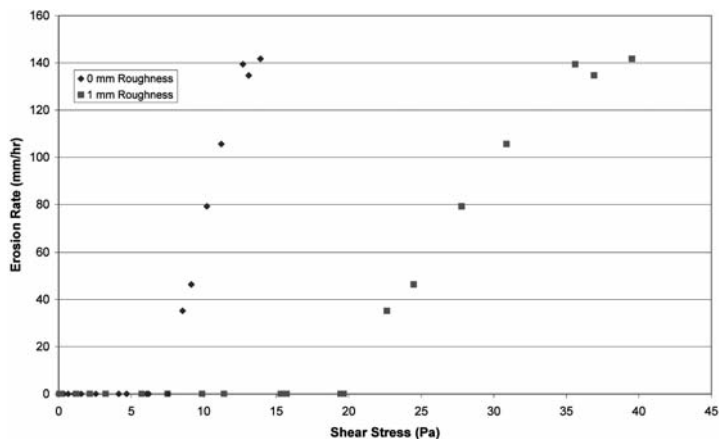


Figure 4. Roughness comparison - Erosion plot for soil obtained from a bridge abutment near Big Sioux River, Flandreau, SD.

Uncertainty is also introduced through the timing of the soil erosion. The operator visually estimates when 1 mm of soil has eroded, but different operators may have different estimates of when the soil has eroded 1 mm because fine-grained soils erode irregularly. If the operator estimates 550 seconds to erode 1 mm of soil, the erosion rate

would be 6.55 mm/hr; however, if the operator estimates 400 seconds to erode 1 mm of soil, the erosion rate would be 9.00 mm/hr. The difference in erosion rates changes the resulting erosion plot.

CONCLUSIONS

In conclusion, the EFA can be a very useful tool as input for designing bridges. It is a simple method for calculating the critical shear stress and EFA plot by using a relatively undisturbed, site-specific soil sample, but the uncertainties are present in the current testing procedure. The unknown roughness value is a critical value that must be determined accurately in order to get a representative critical shear stress and EFA plot for the soil sample.

Because the roughness value is unknown, an estimate must be used for the value in order to calculate the friction factor, f . Figure 4 shows the effects of different roughness value estimates, ϵ , on the critical shear stress and the EFA plot. By varying the ϵ value, a wide variety of plots can be produced.

Further research is needed to find an effective procedure to calculate the roughness value and correct for the uncertainties.

ACKNOWLEDGEMENTS

This study was funded by the South Dakota Department of Transportation (SDDOT) and the Mountain-Plains Consortium (MPC). The support of SDDOT and MPC is gratefully acknowledged.

REFERENCES

1. Briaud, J.-L., Chen, H.C., Li, Y., Nurtjahyo, P., and Wang, J. "SRICOS-EFA Method for Complex Piers in Fine-Grained Soils." *Journal Of Geotechnical And Geoenvironmental Engineering*, ASCE, Vol. 130. No. 11. November (2004): 1180-1191.
2. Briaud, J.-L., Ting, F., Chen, H.C., Gudavalli, R., Perugu, S., Wei, G. "SRICOS: Prediction of Scour Rate in Cohesive Soils at Bridge Piers." *Journal Of Geotechnical And Geoenvironmental Engineering*, ASCE, Vol. 125. No. 4. April (1999): 237-246.
3. Briaud, J.-L., Chen, H.C., Kwak, K.W., Han, S.W., Ting, F. "Multiflood and Multilayer Method for Scour Rate Prediction at Bridge Piers." *Journal Of Geotechnical And Geoenvironmental Engineering*, ASCE, Vol. 127. No. 2. February (2001b): 114-125.
4. Ting, F., Briaud, J.-L., Gudavalli, R., Perugu, S., Wei, G. "Flume Tests for Scour in Clay at Circular Piers." *Journal of Hydraulic Engineering*, ASCE, Vol. 127. No. 11. November (2001): 969-978.
5. Briaud, J.-L., Ting, F., Chen, H.C., Cao, Y., Han, S.W., Kwak, K.W. "Erosion Function Apparatus for Scour Rate Predictions." *Journal Of Geotechnical And Geoenvironmental Engineering*, ASCE, Vol. 127. No. 2. February (2001a): 105-113.

Fatigue Analysis of an Inline Skate Axel

Authors: Garrett Hansen, Mike Woizeschke
Faculty Sponsor: Dr. Shanzhong (Shawn) Duan
Department: Mechanical Engineering

ABSTRACT

In this paper, an inline skate axel is analyzed based on fatigue and economic principles for four different materials. The loading scenario on the axel of the inline skate is derived and broken down to a maximum shear stress that must be less than the maximum fatigue stress of the axel material. A fatigue analysis using Goodman line diagrams is applied to axels made of aluminum, titanium, nylon, and PVC. The material strengths are then compared to the loading requirements and determined whether they would be sufficient for an axel material. Finally, the prices are compared to verify the selection of the cheapest and structurally stable axel material.

INTRODUCTION

Inline skates are a common piece of equipment seen everyday when the summer months roll around. Manufacturers produce thousands of pairs of inline skates a year and are always looking for ways to generate cost savings. Within each pair of inline skates there contains four sets of axels which are mainly constructed of an aluminum-based alloy. If a replacement material could be found that provides enough strength to withstand the system loading and is cheaper, such cost savings could be generated. Material strength properties are extremely important because if any of the axels were to fail during the use of the product, the manufacturers would be at fault and the operator may sustain injuries.

The first thing that needs to be performed is breaking down the whole inline skate to just the single axel and the loading that is present on the component. Figure 1 shows how the initial maximum force gets evenly divided onto all four axels. Since the loading is predominately shearing, a shearing analysis is the appropriate method to determine maximum loading scenarios. Once this analysis is completed material selection can commence.

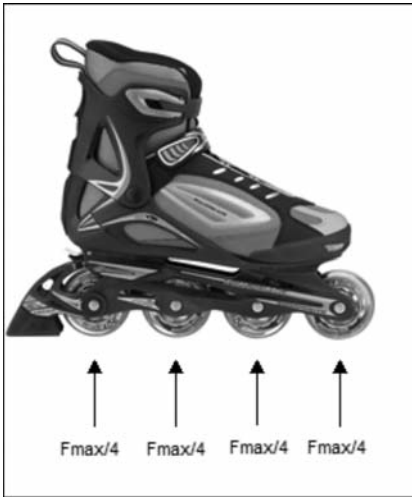


Figure 1. Reaction Forces of an Inline Skate

When selecting materials as a substitute for the current application the Goodman line diagram is a very useful visual to help determine how much stress a material can take for a given dynamical loading. The Goodman line diagram uses the yielding line, the fatigue line, and the application line to produce an intersection point which represents the point of operation under peak loading conditions. Clearly, different materials are capable of producing different maximum operating stresses. These maximum operating points will be found for aluminum, titanium, nylon, and PVC. After the materials are compared to the maximum loading scenario, a selection will be made based first on structural integrity (being able to withstand the loading) and second by an economic standpoint (being able to produce cost savings from the current setup).

METHODS

The main point of analysis on the axel is the area of fatigue. This is due to the wheels going through a high number of cyclic loadings. The method used to analyze the fatigue on the axel is the fatigue theory with Goodman Line Diagram. To construct a Goodman Line Diagram we need to know specific information about both the material and the loading situation to which the object will be subjected.

First, we take a look at the loading situation. In the use of an inline skate, the average repeated maximum force on the axel would be the weight of the user when the user is on one blade, and the minimum force would be zero. A maximum weight that is set for the inline skate at $F = 400\text{lbs}$ and a safety factor of 1.5 is selected [1]. Since each skate has four axels and the force is transmitted to the axel through the outsides of the

blade, a reasonable assumption was made that one axel could be modeled with amplitude of $F/4$ or 100lbs.

The main point of analysis is in the axel of the inline skate. A three dimensional model of the axel is drawn in Pro-E™ as shown in Figure 2.



Figure 2. Pro-E™ Model of the Axel

Based on the model in Figure 2, its simplified model is shown in Figure 3. The axel of the inline skate can be simplified as a cylinder since diameter difference is small. The load is distributed as shown in the same figure.

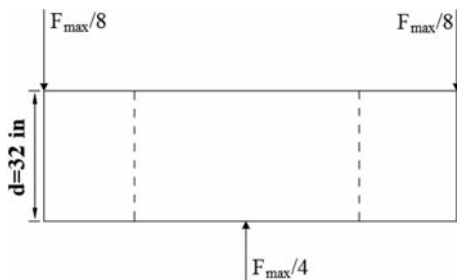


Figure 3. Load Distribution on the Simplified Model

With the loading and the simplified model of the axle, the stresses on the axle are calculated. The stress on the axle can be found by using the basic definition of shearing stresses with consideration of safety factor. The equation for shearing stress is shown in equations 1 and 2.

$$SF = \frac{\text{design overload}}{\text{normal load}} \tag{1}$$

and

$$\sigma = SF \frac{F}{A} \tag{2}$$

where,

- σ = Stress for design overload
- SF = Safety factor
- F = Force
- A = Cross-sectional area

Using a cross-sectional area of 0.0804in^2 and the values for the force $\frac{F_{\text{max}}}{8}$ and SF = 1.5 a stress of 0.993 ksi is obtained. This is the stress that any material used to make this

part will meet under the maximum force. With the minimum force being zero the minimum stress will also be zero. From these two known stresses, a sine wave can be used to model the cyclic loading scenario of the axel as shown in Figure 4.

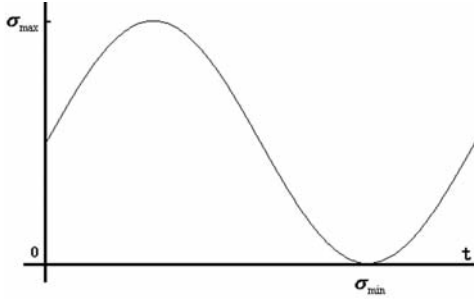


Figure 4. Cyclic Loading Diagram of the Axel

Material properties that need to be known are the yielding strength and the ultimate strength. These properties can be found in a number of references. The values used in this paper are from reference [1]. The Goodman Line diagram is highly dependent on a value called the endurance limit or fatigue strength, S_n , of the selected material. The calculation of the endurance limit depends on several correction factors such as the surface condition, size, loading situation, temperature, and the expected reliability. The following equation shows their relationship:

$$S_n = S'_n C_L C_G C_S C_T C_R \quad (3)$$

where

S_n = fatigue strength of materials

S'_n = standard fatigue strength

C_L = load factor

C_G = gradient factor

C_S = surface factor

C_T = temperature factor

C_R = reliability factor.

The criteria and values for these correction factors can be found in [1]. Before the equation (3) could be used, the Standard Fatigue Strength S'_n has to be calculated as follows:

$$S'_n = 0.5S_u \quad (4)$$

where

S_u = ultimate strength of materials.

The standard life calculation is for a life span of 10^6 cycles. This is a very high number of cycles that can be considered to be infinite for the life of the inline skate.

Next based on fatigue theory and the loads applied on the shaft, the mean stress, σ_m , and the alternating stress, σ_a , will be calculated for the Goodman Line diagram. Since the

loading for the system is from zero to a maximum load the alternating stress and the mean stress are equal. Both are expressed as follows:

$$\sigma_a = \frac{(\sigma_{MAX} - \sigma_{MIN})}{2} \tag{5}$$

and

$$\sigma_m = \frac{(\sigma_{MAX} + \sigma_{MIN})}{2} \tag{6}$$

where,

- σ_a = Alternating stress
- σ_m = Mean stress
- σ_{max} = Maximum stress
- σ_{min} = minimum stress.

Since all the variables are known, the Goodman Line diagram can be constructed. A Goodman line diagram consists of two axes where the horizontal axis represents σ_m , and the vertical axis σ_a with the unit ksi for both. On the horizontal axis the values of the yield strength and the ultimate strength are plotted, then on the vertical axis the yield strength is plotted again as well as the endurance limit. A line is then drawn connecting the yield strength points on the vertical and horizontal axis. This line is called the yielding line. Next a line is drawn from the ultimate strength point on the horizontal axis to the endurance limit point on the vertical axis, which is called the Goodman line for the infinite life cycles. Further, the load line is drawn from the zero point outward with a slope that is equal to the alternating stress divided by the mean stress for the design application. Since the alternating stress equals the mean stress, the load line goes from the zero point at an angle of 45 degrees. The Goodman Line diagram can be seen in Figure 5.

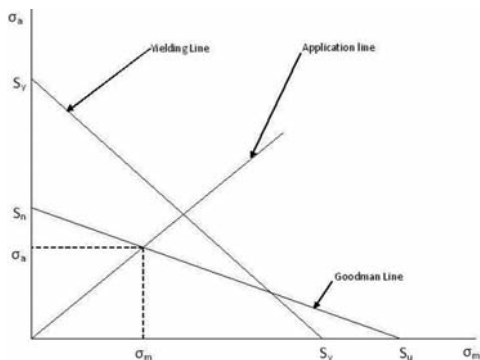


Figure 5. General Setup of Goodman Line Diagram

Now that the Goodman Line diagram is made it must be interpreted. The interpretation starts with finding where the load line intersects the Goodman line and the yielding line. If the load line intersects the yielding line first, then yielding of the material is the main

concern. If the load line intersects the Goodman line before the yielding line, then fatigue is the main area of concern. From the point that the load line intersects the Goodman line we can find the maximum stress that can be handled by the material for the 10^6 life. Since our load line is at 45 degrees it does not matter which axis you take the reading for value of stress because they will be equal. The value that is read off the graph is the maximum fatigue stress that can be put on this material and expect that the material satisfies the fatigue requirements.

Most raw materials are priced on a per pound basis. This requires that the volume of the axel must be found and then the weight of the axel must be found for proper analysis of the cost benefits. From the model of the axel we can figure that the volume is 0.108 in³. The equation used for calculating the weight from the volume and material density can be shown in the following:

$$\text{where} \quad W = V\rho \quad (7)$$

$$\begin{aligned} W &= \text{weight (lbs)} \\ V &= \text{volume (in}^3\text{)} \\ \rho &= \text{density (lbs/in}^3\text{)} \end{aligned}$$

RESULTS

Using the Goodman Line diagramming method described previously, aluminum is the first material to be considered since the current material for the inline skate axels are mainly made of an aluminum alloy. This will give a base comparison point for the other three materials. Figure 6 below is the graphical representation of the Goodman Line diagram for aluminum. The operating point for aluminum under our zero-max loading is where the application line intersects the Goodman line. Reading to one of the axis (σ_m or σ_a) on the graph, the maximum stress of the material for the application is found. For aluminum this value turned out to be 15.5 ksi. Because this value is above the max loading scenario stress, a validation for using this material has been achieved but at a cost of around \$2.00/pound (material price may fluctuate).

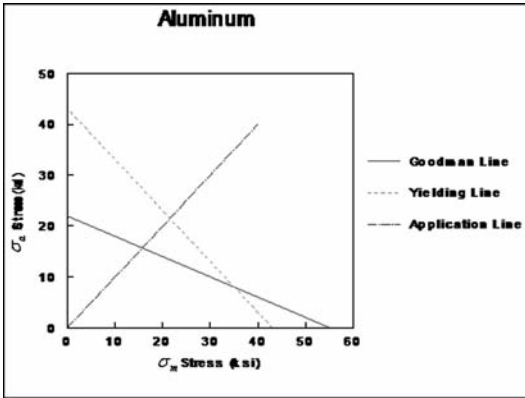


Figure 6. Goodman Line Diagram for Aluminum

Once again using the Goodman Line diagram for titanium, Figure 7 shows that the material stress is around 34 ksi. This is well over the requirement of around 1.0 ksi and thus could be a viable material to use. However; the cost of titanium is approximately \$25.50/pound, so producing the axels out of this material is not a wise choice especially in the case of trying to generate cost savings.

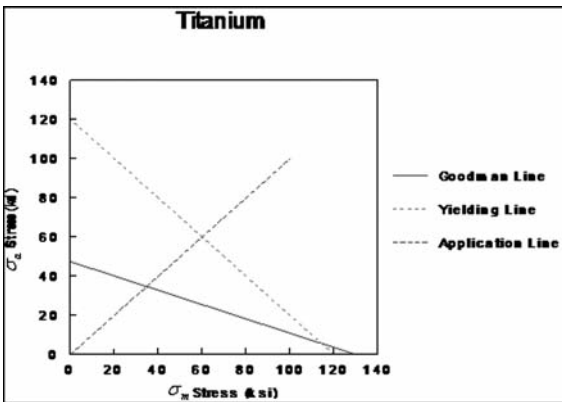


Figure 7. Goodman Line Diagram for Titanium

Using the Goodman Line diagram as shown in Figure 8 for nylon shows that the material stress is far less than that of the previous two materials. The nylon stress was calculated to be 4 ksi. Once again this is large enough to withstand the loading situation

and it also provides cost savings since the price of nylon is only \$1.64/pound of material. Comparing this to aluminum, that's a saving of around 36 cents per pound of material used on the inline skates.

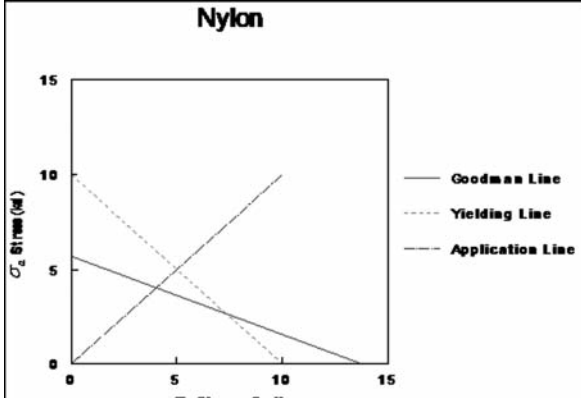


Figure 8. Goodman Line Diagram for Nylon

Finally there is PVC to consider. Running the Goodman Line analysis on this material provides some promising data. Figure 9 below shows that like the other three materials selected, it can withstand the loading stresses, too. PVC is calculated to have a material strength of around 2.1 ksi which is still a little more than double of the required strength for the loading. The cost of PVC per pound is only about 41 cents. This equates to a cost savings of around \$1.59/pound when compared to aluminum.

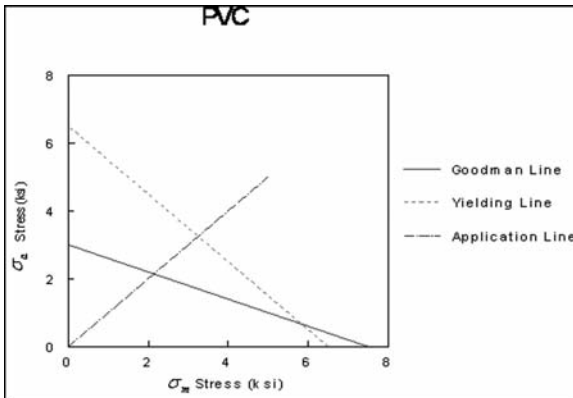


Figure 9. Goodman Line Diagram for PVC

DISCUSSION

As you can see all of the materials that are used in this analysis would work. The values calculated are shown in Table 1.

Table 1. A Comparison of Load Capacity and Costs of Four Materials

Material	Nylon	PVC	Aluminum	Titanium
Infinite Life (ksi)	4	2.1	15.5	34
Price per lbs (\$/lbs)	1.64	0.41	2.00	25.49
Density (lbs/in ³)	0.001268	0.001501	0.1	0.16
Cost of Part Material (\$)	0.000225	0.000066	0.021600	0.440467

Assuming that the axels can be manufactured in the same way, it can be reasoned that the PVC axel would be the best choice for cost saving. The material cost savings of the PVC over aluminum is around 327%. The savings per pair of inline skate would be about \$0.172. This may not seem like a lot but if the company only produced 100,000 pairs of inline skates with PVC axels they would save \$17,200 over the aluminum axels.

The previous values are assuming that the manufacturing for the plastics are the same as the metals but the plastics that were selected could both be used in injection molding techniques. Since injection molding normally makes a very high amount of parts relatively quickly, it can be assumed that time as well as material cost could be saved with the use of plastic.

LIMITATIONS

There are some limitations on the numbers attained above. The raw material costs are just a snapshot in time and all prices could fluctuate. So what might be cheaper now might not be cheaper later.

REFERENCES

- [1] Juvinall, R. C. and Marshek, K. M. Fundamentals of Machine Components Design. 2006. Wiley, NJ.
- [2] Palin, G.R. Plastics for Engineers. 1967. New York, NY